International Journal of GEOMATE, April 2023, Vol. 24, Issue 104, pp.19-26
ISSN: 2186-2982 (P), 2186-2990 (O), Japan, DOI: https://doi.org/10.21660/2023.104.3666
Geotechnique, Construction Materials and Environment

STABILISATION OF DEGRADED CLAY SHALE WITH THE GEOPOLYMER INJECTION METHOD

*Sumiyanto[1,3], Sri Prabandiyani Retno Wardani[1] and Agus Setyo Muntohar[2]

[1]Engineering Faculty, Diponegoro University, Indonesia
[2]Engineering Faculty, Universitas Muhammadiyah Yogyakarta, Indonesia
[3]Engineering Faculty, Jenderal Soedirman University, Indonesia

*Corresponding Author, Received: 25 Oct. 2022, Revised: 31 Jan. 2023, Accepted: 26 Feb. 2023

ABSTRACT: Geopolymer injection is a method for increasing the strength of degraded clay shale. Clay shale is a type of mud rock with low durability. Samples of clay shale were exposed to weather changes and in an open field to observe weathering and degradation. A series of laboratory experiments was also conducted on reconstituted clay shale specimens. The primary objective of this research was to investigate the factors influencing the distribution of geopolymer injected into compacted clay shale. The strength index of stabilised clay shale was examined in terms of unconfined compressive strength. Soil density was varied with three relative compaction values, namely, 0.75, 0.85 and 0.95, of the maximum dry density, which correspond to porosity of 0.54, 0.48 and 0.42, respectively. Geopolymer was varied in four activator-fly ash ratios, namely, 0.5, 0.75, 1, and 1.25. An empirical equation was developed for calculating the volume of the injected geopolymer and the radius of the soil–grout column. This equation is a function of injection pressure, duration, geopolymer viscosity and air void porosity. The unconfined compressive strength of the compacted clay shale increased up to five times after geopolymer grouting. The contribution of geopolymer injection is correlated with the size or volume of the soil–grout column.

Keywords: Geopolymer, Clay shale, Injection, Soil–grout column

1. INTRODUCTION

Clay shale has been classified as a low-durability rock. Weathering induces cracks, eventually causing clay shale to degrade into fragments and fully soften when wet [1]. Weathering cause rapid decrease in the strength of clay shale [2]. Failures may occur years after fissures were formed due to exposure to weathering and the resultant decreased strength. Consequently, the degradation of clay shale can cause construction damage [3]. Even where pavement structure covers the soil, problems can arise from sub-surface weathering after the compaction of clay shale as a road subgrade [4].

Degraded clay shale requires stabilisation to increase shear strength. Soil stabilisation with cement has long been applied to improve the strength of weathered clay shale [5]. However, cement production generates carbon emissions, which affect the environment and human lives. This situation has encouraged the innovation and development of alternative materials. During their early development, geopolymers were intended as cement substitutes in concrete [6]. In general, geopolymers are composed of activators and binders. Aluminosilicate materials and alkaline solutions are commonly used as geopolymers. An alternative method is to use low-cost aluminosilicate material waste, e.g. fly ash (FA) as binders [7]. For alkaline activators, sodium (or potassium) hydroxide and sodium (or potassium) silicate are customarily used [8].

The use of geopolymers has been explored to stabilise clayey soil [9]. The utilisation of geopolymers as grouting materials in soil has been developed through a deep mixing method in soft soil [10-11]. However, research on geopolymer grouting in clay shale has been scarce. Under intact condition, clay shale has a low porosity of around 0.20, but its porosity will increase to 0.54 when clay shale is degraded [12]. The large porosity under degraded condition provides an opportunity for injection. Therefore, research on geopolymer injection is necessary to explore the feasibility of its further application to highway pavement structures. The current study investigates the influence factors of geopolymer injection distribution in compacted clay shale and examines the unconfined compressive strength (q_u). The q_u of the geopolymer injection method was compared with that of the geopolymer–soil mixing method. This research can contribute to improving the subgrade and pavement structure restoration of existing highways.

2. RESEARCH SIGNIFICANCE

The deterioration of clay shale under the road or other infrastructure potentially occurs due to weathering process. To prevent the failure of adjacent infrastructure, it is essential to improve degraded clay shale. Injection grouting using fly

ash-based geopolymer is a potential technique and substance for addressing this problem. Moreover, the use of fly ash as a geopolymer is an effort to utilize waste to encourage the development of environmentally friendly building materials. Concerning this issue, a comprehensive laboratory test was conducted to determine the effectiveness of this method.

3. EXPERIMENTAL PROGRAMME

3.1 Materials

Clay shale was collected from Limbasari in Purbalingga, Central Java. The soil sample was classified as high plasticity clay, with its index properties listed in Table 1. The principal clay mineral in the soil sample was smectite (~51%), with 9% illite, as determined via X-ray diffraction (XRD) analysis. Smectites shrink upon drying and swell upon wetting [13]. The key chemical elements of clay shale as determined via X-ray fluorescence (XRF) were SiO_2 (53%), Al_2O_3 (20%), CaO (15%) and Fe_2O_3 (7%).

Fly ash (FA) is an abundant waste material in PJB Tanjungjati coal-fired power plant (Fig. 1a). The current research freely collected FA from PJB Tanjungjati in Jepara, Central Java. The major chemical elements of FA are SiO_2 (51%), Al_2O_3 (29%) and Fe_2O_3 (11%). The summation of these elements is 91%, which is classified under class F in accordance with ASTM C618 [14]. Class F FA is generally non-self-cementing and contains 2%–6% CaO. Accordingly, its use requires additional lime to achieve self-cementing properties [15]. FA was enriched with quartz (50%), mullite (33%) and magnetite (17%) minerals. Geopolymers were made from FA with an alkaline activator mixture. The activator was created with a mix of 10 M NaOH and Na_2SiO_3 in a ratio of 1:1. The density (γ_g), viscosity (μ_g) and initial setting time of each activator–FA ratio (f) are presented in Table 2. The μ_g was determined using Zahn Cup # 4 as required in ASTM-D4212-99 [16].

Table 1 Index properties of the soil sample

Parameter	
Specific gravity, Gs	2.52
Maximum dry density, MDD (kN/m^3)	15.2
Optimum moisture content, (%)	18.6
Liquid limit, LL (%)	51.1
Plastic limit, PL (%)	24.4
Plasticity index, PI (%)	26.7

3.2 Preparation of Specimens

Dry clay shale lumps (Fig. 1b) were degraded using the jar method, which involved heating the material for 24 h at 100 °C before immersing it in water. In addition, fragmented clay shale was sieved through no. 4 mesh (< 4.75 mm), as shown in Fig. 1c. Under this condition, clay shale is in a fully degraded state [17].

Table 2 Properties of geopolymer

Activator-to-FA ratio, f	Properties		
	Density, γ_g (g/cm^3)	Viscosity, μ_g (mPa.s)	Initial setting time (min)
0.50	1.99	5,350	729
0.75	1.92	1,519	1,850
1.00	1.85	605	2,100
1.25	1.79	309	2,900

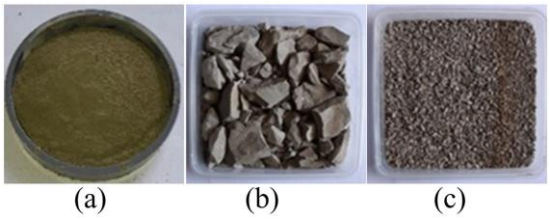

Fig. 1 Materials: (a) FA, (b) dry clay shale fragments and (c) degraded clay shale (passed no. 4 sieve)

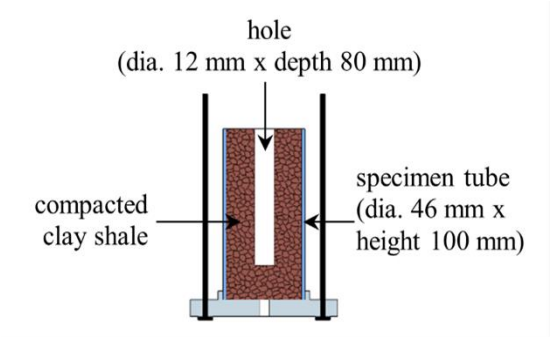

Fig. 2 Schematic and dimension of specimen

The soils were compacted at the optimum moisture content to obtain the designation densities. The specimens were prepared in three densities determined, by relative compaction (R_c), i.e., 0.75, 0.85, and 0.95. The compacted specimens correspond to porosity (n) is 0.54, 0.48 and 0.42. The soil was compacted statically using a hydraulic jack in polyvinyl chloride (PVC) tubes with two diameters of 46 and 105 mm, with a height of 100 mm for each specimen, as illustrated in Fig. 2. A hole was prepared at the centre of the specimen as the injection point. For samples with a diameter of 46 mm, the hole size was 12 mm in diameter and 80 mm in depth, and for samples with a diameter of 105 mm, the holes were made with three diameters

Table 3 Testing design of geopolymer injection

Tube diameter (mm)	Hole diameter (mm)	Relative compaction, R_c	Activator-to-FA ratio, f				Injection pressure, p (kPa)			Injection duration, t (min)					
			0.5	0.75	1	1.25	50	100	150	0.5	1	2	5	10	20
46	12	0.75	●	●	●	●	○	●	○	○	○	○	○	○	●
46	12	0.85	●	●	●	●	●	●	●	●	●	●	●	●	●
46	12	0.95	●	●	●	●	○	●	○	○	○	○	○	○	●
105	12	0.85	○	○	●	○	○	●	○	○	○	○	○	○	●
105	25	0.85	○	○	●	○	○	●	○	○	○	○	○	○	●
105	38	0.85	○	○	●	○	○	●	○	○	○	○	○	○	●

Note: ○ = not conducted ● = test conducted

of 12, 25 and 38 mm. In addition, as illustrated in Fig. 3, the specimen was mounted on the injection equipment. The geopolymer was injected into the hole under a certain pressure (p) and duration (t) as designed in Table 3. The volume of injected geopolymers (V_i) was calculated based on the subtraction of specimen weight before and after injection, then divided by the geopolymer unit weight.

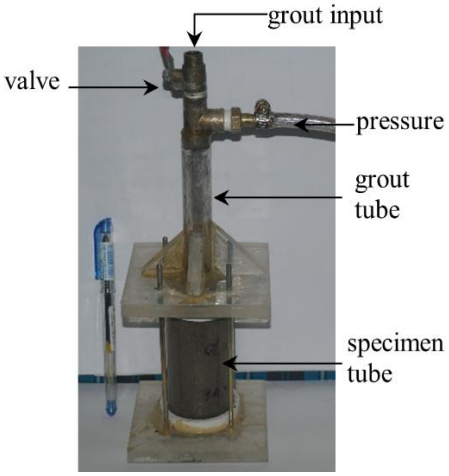

Fig. 3 Specimen mounted on injection equipment

Injection distribution was determined via the jar test method, which was conducted 14 days after geopolymer injection. The samples were immersed in water for 20 min, allowing unreacted or uncemented soil to be dispatched from the cemented soil column. The cemented soil column was weighed to determine its mass (m_a). The column was coated with wax and weighed underwater. Then, mass (m_w) was determined. The volume of the soil–grout column (V_{cg}) was calculated on the basis of the difference between m_a and m_w and divided by the density of water. Injection distribution was determined by the radius of the soil–grout column (R_i), which was calculated on the basis of V_{cg}, assuming that the column had a cylindrical shape.

3.3 Unconfined Compressive Strength Test

The strength of clay shale after geopolymer injection was determined using the q_u test after 7 days of using a displacement rate of 1 mm/mm in accordance with ASTM D2166-06 [18]. The peak axial stress of each specimen was used to determine the value of q_u. For comparison, a second group of q_u testing was also conducted on clay shale stabilised by geopolymer through the mixing method. The specimen was mixed at various R_c, activator-FA ratio and the same geopolymer content as the injection test specimen. In preparing the soil–geopolymer mixtures, geopolymer was added to dry soil in the required proportions and mixed thoroughly. The slurry was transferred into a PVC tube as designed in Table 3 and compacted statically using a hydraulic jack.

4. RESULTS AND DISCUSSION

4.1 Grouted Column

A series sample from the jar test at a R_c of 0.85 with varying activator-FA ratio is shown in Fig. 4. With an increase of activator-FA ratio from 0.5 to 1.25, the soil–grout column radius (R_i) rose from 10.6 mm to 17.9 mm. Geopolymer viscosity (Table 2) increases with increasing activator-FA ratio, and thus, spreading the geopolymer is easier and larger grouting soil is produced. In addition, Fig. 5 shows the combined effects of R_c and activator-FA ratio. It illustrates how R_i is reduced as R_c rises because porosity (n) also decreases when R_c rises. In accordance with classical theory [19], the effects of R_c and activator-FA ratio on R_i are consistent.

The injection test result presented in Fig. 6 shows that the injection rate on R_i is initially high. After a particular time (t = 5 min), the effect of t on R_i is slightly linear or nearly asymptote. During injection, the geopolymer is initiated to fill the air pores. The subsequent process becomes difficult because the pore is partially filled with grout materials. This condition causes a decrease in

injection rate [20]. The effect of pressure (p) on R_i is also illustrated in Fig. 7. The effect of p is slightly linear within the range of 50 to 150, although being higher at p less than 50 kPa. This effect is similar to sandy soil [21].

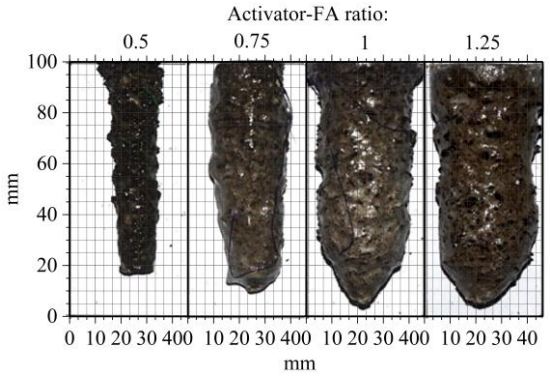

Fig. 4 Soil–grout column profiles with R_c = 0.85 and various activator-FA ratio values

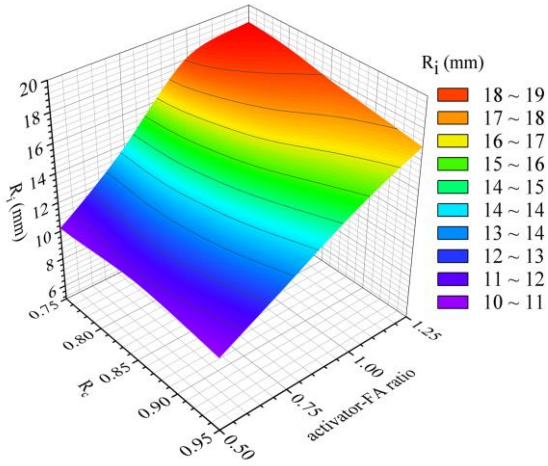

Fig. 5 Radius of the soil–grout column (R_i) for various R_c and activator-FA ratio values

This study also establishes an analytical model for calculating R_i by using experimental data. R_i is represented as a nondimensional parameter. Analysis is performed in two stages: injected volume and injection diffusion or spreading radius. Perret et al. [20] explained that in an unsaturated state, suction makes grouting easier to fill the pores. Under saturated condition, the presence of water inhibits the flow of grouting in the pores. This condition indicates the role of air volume (air void porosity) in the injection process. Based on this consideration, the soil porosity (n) variable is replaced by air void porosity (n_a), which is calculated using Eq. (1), where S is the degree of saturation.

$$n_a = n(1 - S) \quad (1)$$

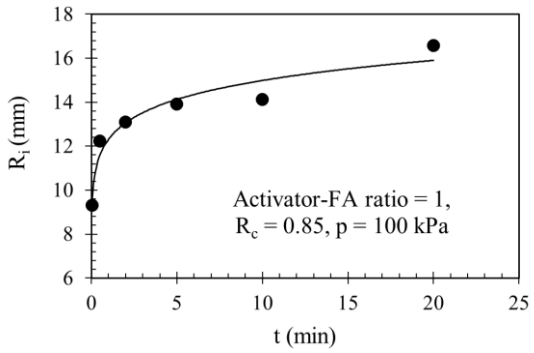

Fig. 6 Effects of duration (t) on grout column radius (R_i)

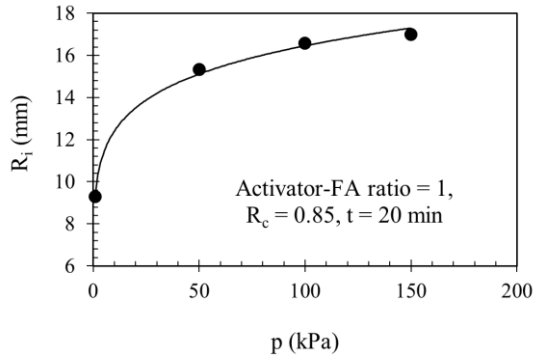

Fig. 7 Effects of pressure (p) on grout column radius (R_i)

In this analysis, the injected volume (V_i) is assumed to be equal to the borehole volume (V_b) and the filled soil pores. The injection process (pressure and time) will initially fill the borehole and propagate to penetrate the surrounding soil through the borehole wall. Furthermore, the injected volume can be written as shown in Eqs. (2) and (3), where A_1 = 0.00509, A_2 = 1.1354 and A_3 = 0.3697. These constants are solved numerically on the basis of experiment data. The V_i calculated using Eq. (3) has a mean absolute percentage error (MAPE) of 8.6% compared with the experimental data. A comparison of the calculated and experimental V_i values is presented in Fig. 8.

$$\frac{V_i - V_b}{V_b} = A_1 (n_a)^{A_2} \left(\frac{p \times t}{\mu_g}\right)^{A_3} \quad (2)$$

$$V_i = V_b \left[1 + A_1 (n_a)^{A_2} \left(\frac{p \times t}{\mu_g}\right)^{A_3}\right] \quad (3)$$

Geopolymer diffusion is determined by the R_i, which is measured via the jar test. The R_i is related to V_i, which is the function of n_a, p, t, and μ_g. The R_i can be written empirically as shown in Eq. (4), where B_1 = 0.01262, B_2 = 0.342 and B_3 = 0.275. These constants are solved numerically on the basis

of the experiment data. The calculated R_i and the experiment R_i are compared in Fig. 9. The relationship in Fig. 9 indicates that the R_i calculated using Eq. (4) is close to the experimental results with a MAPE of 8.3%.

$$R_i = R_b \left[1 + B_1 (n_a)^{B_2} \left(\frac{p \times t}{\mu_g}\right)^{B_3}\right] \quad (4)$$

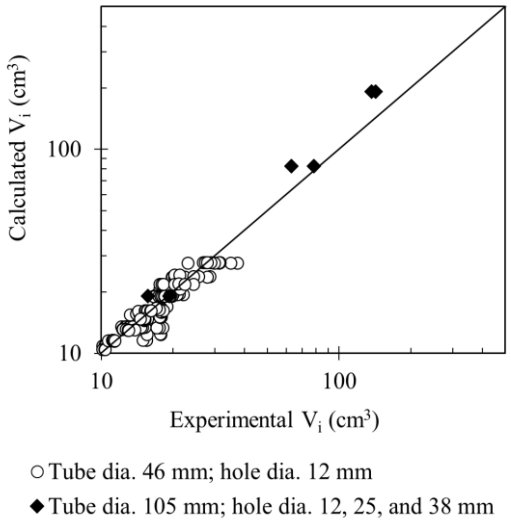

Fig. 8 Comparison of injected volume (V_i) between the calculated and experimental values

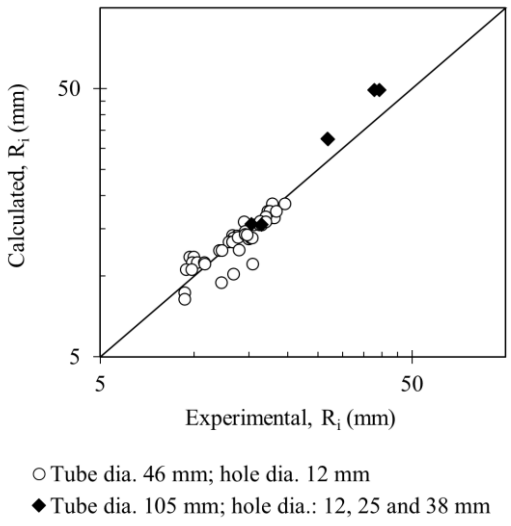

Fig. 9 Comparison of grout column radius (Ri) between the calculated and experimental values

Soga et al. [22] conducted injections into small specimens with a diameter of 50 mm. The result suggested that the boundary of the 50 mm diameter could limit the magnitude and extent of the excess pore water pressure zone, resulting in better grout efficiency. However, specimen boundary may affect V_i and R_i, particularly at a low density and less viscous geopolymer. As a consequence of these boundary conditions, the V_i and R_i equations should be further investigated at more extensive boundary conditions. However, Eqs. (3) and (4) can be used as the bases for equation development, primarily to obtain the A_1, A_2 and A_3 in Eq. (3) and B_1, B_2 and B_3 in Eq. (4) at more oversized circumstances.

4.2 Unconfined Compressive Strength

Unconfined compressive strength tests are conducted to determine the strength (q_u) of the stabilised clay shale. Figure 10 presents the q_u with the variation of activator-FA ratio and R_c. One of the most important variables for determining the q_u of grouted clay shale is f. Figure 10 shows the variation of q_u for the injection and slurry mixing methods. q_u increases proportionally with an increase in f. The strength of cementation contact bonds between soil particles can increase with increasing f. The findings presented in Fig. 10 reveal that activator-FA ratio must develop optimum compressive strength. V_i is physically limited by borehole size, soil pore size and specimen boundary. Grout flow in porous media depends on μ_g and t. Thus, this boundary leads to the optimum compressive strength.

The q_u of the unstabilised clay shale is 37, 104 and 299 kPa for R_c values of 0.75, 0.85 and 0.95, respectively. The contribution of the geopolymer to increasing q_u can be measured by the strength index (Δq_u), which is determined as Eq. (5).

$$\Delta q_u = \frac{q_{u(stabilized)} - q_{u(unstabilized)}}{q_{u(unstabilized)}} \quad (5)$$

A higher Δq_u indicates a higher strength development of the geopolymer in the compacted clay shale, as shown in Fig. 11. The contribution of geopolymer injection increases up to five times at loose clay shale (R_c = 0.75) but is less significant at dense clay shale (R_c = 0.95), although q_u is higher than loose clay shale. The results show that soil density controls the strength development of the geopolymer in compacted clay shale. For soil with R_c = 0.75, the greater the value of f, the higher Δq_u is obtained. However, the optimum value is not obtained. At R_c = 0.85 and R_c = 0.95, increasing activator-FA ratio from 1 to 1.25 increases slightly or tends to be an asymptotic increment of q_u (Fig. 10). The results imply that an optimum activator-FA ratio is likely less than 1.25. Some studies on geopolymer mortar have found that the optimum value of activator-FA ratio is within the range of 0.5–0.6 [23]. An inadequate amount of alkaline

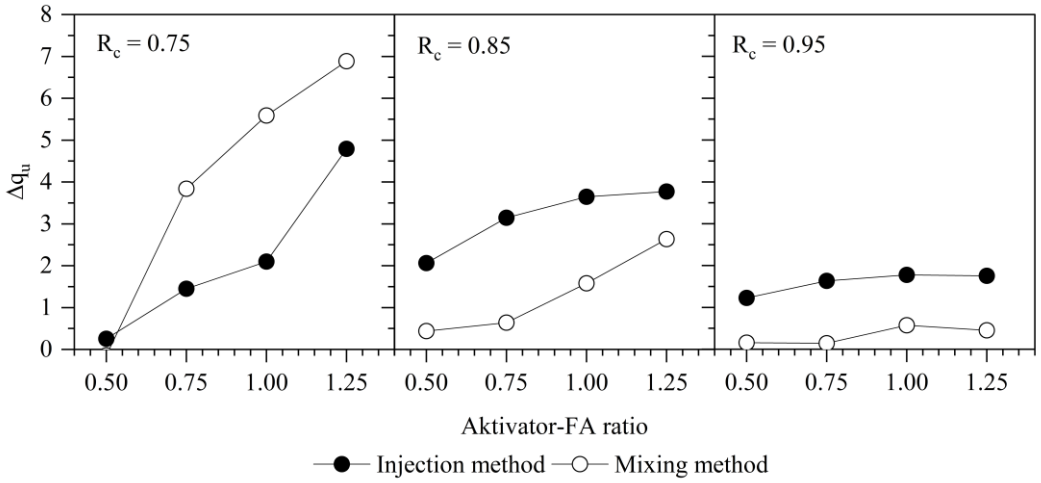

Fig. 10 Effects of R_c and activator-FA ratio on q_u by using the injection and mixing methods

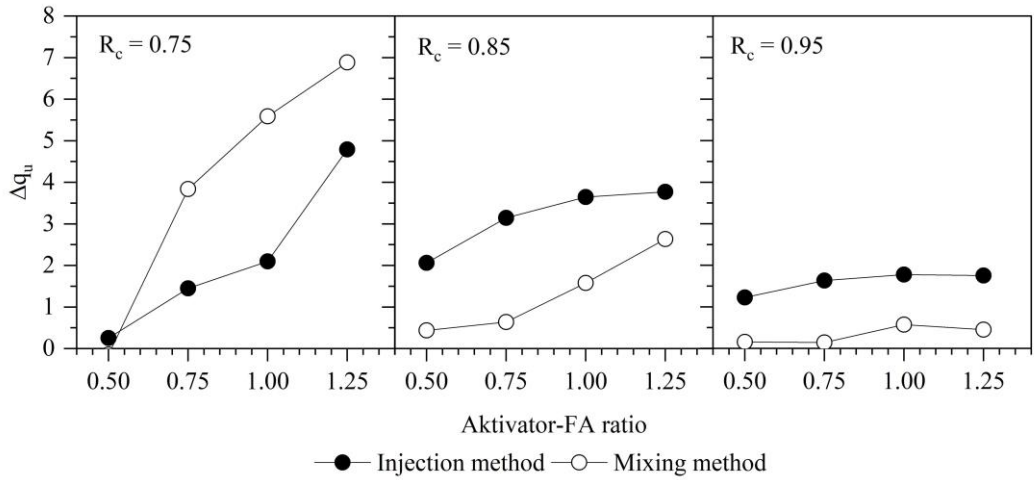

Fig. 11 Effects of R_c and activator-FA ratio on Δq_u by using the injection and mixing methods

activator for dissolving FA particles may decrease q_u. As a result of unreacted FA particles, a weak geopolymer mortar with a nonhomogeneous structure is likely to form. By contrast, using a higher activator-FA ratio value over the optimum value can reduce q_u. An overabundance of activators inhibits the geopolymerisation process [24].

4.3 Comparison of the Injection and Mixing Methods

The q_u of the injection method is also compared with that of the mixing method, as shown in Fig. 10. In general, q_u increases with an increase in f. As shown in Figure 10, for R_c = 0.75, the q_u of the mixing method is more significant than that of the injection method. FA acts as a binder. The higher the amount of FA, the stronger the bond and the higher the compressive strength. The activator functions to activate FA, and the amount required is about 0.35 of the weight of FA [26]. Within this range of values, however, μ_g is high, making it difficult to achieve in the injection process. The injection process requires a high f, but the excessive use of activators can decrease compressive strength due to constraints in the geopolymerisation process and the emergence of air voids [10].

For R_c values of 0.85 and 0.95, Fig. 10 shows that the q_u of the mixing method is lower than that of the injection method. The geopolymer is concentrated in the borehole and its surroundings to form a grouting column in the injection method. At denser soil, the size and volume of the void are smaller than those at looser soil. This condition increases the clogging effect [27], wherein FA that has filled the pores will inhibit the next injection process. By contrast, the geopolymer is supposed to spread evenly in the mixing method. The binder content plays a central role in geopolymer for improving clay by soil mixing [11]. In terms of FA percentage,

the higher the FA content of the mixtures, the better the performance of the mixture in terms of strength development [10]. The FA content of the soil mixing method is about 6%–8% of the dry weight of soil for dense soil (R_c = 0.85 and 0.95). In accordance with other studies, approximately 15% of FA exerts the optimum effects on soil stabilisation [9]. This condition is probably the cause of the lower q_u of the mixing method compared with that of the injection method. However, the FA content for loose soil (R_c = 0.75) is close to the optimum, which is about 10%–13%, such that the q_u of the mixing method is higher than that of the injection method.

5. CONCLUSIONS

A series of laboratory investigations has been conducted to study the soil–grout size, strength and microstructure of geopolymer-stabilised clay shale. The conclusions drawn are as follows.

1. Injected volume (V_i) is a function of activator-to-FA ratio (f), injection pressure (p), length (t), viscosity (μ_g) and air void porosity (n_a) The radius of spreading is related to Eq. (4). The radius of the soil–grout column (R_i) calculated using Eq. (4) is close to the experimental results, with a mean error of 8.3%.
2. The unconfined compressive strength (q_u) is proportional to the density of clay shale. The initial density of the specimen influences unconfined compressive strength significantly. Denser soil has greater unconfined compressive strength. In addition, the unconfined compressive strength increases as activator-FA ratio increases.
3. The unconfined compressive strength (q_u) of the compacted clay shale increases up to five times via geopolymer grouting. This scenario occurs in clay shale with relative compaction (R_c) is 0.75 and geopolymer with as activator-FA ratio is 1.25. The contribution of geopolymer injection corresponds to soil–grout column size.
4. The mixing method with low FA content is less effective than the injection method in increasing the unconfined compressive strength of compacted clay shale. However, the mixing method is more effective than the injection method at the FA content in the optimum zone.

6. ACKNOWLEDGEMENT

The authors gratefully acknowledge the financial support of the Ministry of Education, Culture, Research and Technology of the government of the Republic of Indonesia for the doctoral scholarship (first author). Supporting from the Universitas Muhammadiyah Yogyakarta is also highly appreciated (third author)

7. REFERENCES

[1] Supandi Z.Z., Sukiyah E., and Sudradjat A., The Correlation ff Exposure Time and Claystone Properties at The Warukin Formation Indonesia, Int. J. GEOMATE, Vol. 15, Issue 52, 2018, pp. 160–167.

[2] Gautam T.P., and Shakoor A., Slaking Behavior of Clay-Bearing Rocks During a One-Year Exposure to Natural Climatic Conditions, Eng. Geol., Vol. 166, 2013, pp. 17–25.

[3] Miščević P., and G. Vlastelica G., Impact of weathering on slope stability in soft rock mass, J. Rock Mech. Geotech. Eng., Vol. 6, Issue 3, 2014, pp. 240–250.

[4] Muhrozi and Wardani S.P.R, Problem of High Embankment on Clay Shale at Semarang-Ungaran Toll Road STA 5 +500 to 6 +300, in Geotechnical Engineering for Disaster Mitigation and Rehabilitation and Highway Engineering, 2011, pp. 159–171.

[5] Diana W., Hartono E., and Muntohar A.S, The Permeability of Portland Cement-Stabilized Clay Shale, IOP Conf. Series: Materials Science and Engineering, Vol. 650, Issue. 12019, 2019, pp. 1-6

[6] Hassan A., Arif M., and Shariq M., Use of Geopolymer Concrete for A Cleaner and Sustainable Environment - A Review of Mechanical Properties and Microstructure, J. Clean. Prod., Vol. 223, 2019, pp. 704–728.

[7] Sasui S., Kim G., Nam J., Koyama T., and Chansomsak S., Strength and Microstructure of Class-C Fly Ash and GGBS Blend Geopolymer Activated in NaOH & NaOH + Na2SiO3, Materials, Vol. 13, Issue 1, 2019, pp. 1-15

[8] Juengsuwattananon K., Winnefeld F., Chindaprasirt P., and Pimraksa K., Correlation Between Initial SiO_2/Al_2O_3, $Na2O/Al_2O_3$, Na_2O/SiO_2 and H_2O/Na_2O Ratios on Phase and Microstructure of Reaction Products of Metakaolin-Rice Husk Ash Geopolymer, Constr. Build. Material, Vol. 226, 2019, pp. 406–417.

[9] Singhi B., Laskar A.I., and M. A. Ahmed M.A, Investigation on Soil–Geopolymer with Slag, Fly Ash and Their Blending, Arab J. Sci. Eng., Vol. 41, Issue 2, 2016, pp. 393–400.

[10] Cristelo N., Glendinning S., Fernandes L., and Pinto A.T., Effects of Alkaline-activated Fly Ash and Portland Cement on Soft Soil Stabilisation, Acta Geotech., Vol. 8, Issue 4, 2013, pp. 395–405.

[11] Arulrajah A., Yaghoubi M., Disfani M.M., Horpibulsuk S., Bo M.W., and Leong M., Evaluation of Fly Ash and Slag-based Geopolymers for The Improvement of A Soft

Marine Clay by Deep Soil Mixing, Soils Found., Vol. 58, Issue 6, 2018, pp. 1358–1370.
[12] Kanji M.A., Critical Issues in Soft Rocks, J. Rock Mech. Geotech. Eng., Vol. 6, Issue 3, 2014, pp. 186–195.
[13] Schulze D.G., Clay Minerals, in Encyclopedia of Soils in The Environment, D. Hillel, Oxford, Elsevier, 2005, pp. 246–254.
[14] ASTM C618-08a, Standard Specification for Coal Fly Ash and Raw or Calcined Natural Pozzolan for Use in Concrete, ASTM International, West Conshohocken, Pennsylvania, 2008.
[15] ASTM D5239-04, Standard Practice for Characterizing Fly Ash for Use in Soil Stabilization. West Conshohocken, Pennsylvania, ASTM International, 2004.
[16] ASTM D4212-99, Standard Test Method for Viscosity by Dip-Type Vocosity Cup, ASTM International, West Conshohocken, Pennsylvania, 2005.
[17] Dearman W.R., Weathering Classification in The Characterisation of Rock for Engineering Purposes in British Practice, Bulletin of the International Association of Engineering Geology, Vol. 9, 1974, pp. 33–42.
[18] ASTM D2166/D2166M-16, Standard Test Method for Unconfined Compressive Strength of Cohesive Soil, ASTM International, West Conshohocken, Pennsylvania, USA, 2016.
[19] Hou F., Sun K., Wu Q., Xu W., and Ren S, Grout Diffusion Model in Porous Media Considering the Variation in Viscosity with Time, Adv. Mech. Eng., Vol. 11, Issue 1, 2019, pp. 1–9.
[20] Perret S., Khayat K.H., and G. Ballivy G., The Effect of Degree of Saturation of Sand on Groutability - Experimental Simulation, Ground Improvement, Vol. 4, Issue 1, 2000, pp. 13–22.
[21] Wang Q., Wang S., Sloan S.W., Sheng D., and Pakzad R., Experimental Investigation of Pressure Grouting in Sand, Soils Found., Vol. 56, Issue. 2, 2016, pp. 161–173.
[22] Soga K., Au K.A., Jafari M.R, and Bolton M.D., Discussion: Laboratory Investigation of Multiple Grout Injections Into Clay, Géotechnique, Vol. 55, Issue 3, 2004, pp. 257–258.
[23] Hadi M.N.S., Al-Azzawi M., and Yu T., Effects of Fly Ash Characteristics and Alkaline Activator Components on Compressive Strength of Fly Ash-based Geopolymer Mortar, Constr. Build. Material, Vol. 175, 2018, pp. 41–54.
[24] Reig L., Soriano L., Borrachero M.V., Monzó J., and Payá J., Influence of Ahe Activator Concentration and Calcium Hydroxide Addition on The Properties of Alkali-activated Porcelain Stoneware, Constr. Build. Material, Vol. 63, 2014, pp. 214–222.
[25] Dano C., Hicher P.Y., and Tailliez S., Engineering Properties of Grouted Sands, J. Geotech. Geoenvironmental Eng., Vol. 130, Issue 3, 2004, pp. 328–338.
[26] Bakri A.M.M., Kamarudin H., Karem O.A.K.A., Ruzaidi C.M., Rafiza A.R., and Norazian M.N., Optimization of Alkaline Activator/Fly Ash Ratio on The Compressive Strength of Manufacturing Fly Ash-based Geopolymer, Appl. Mech. Material, Vol. 110–116, 2012, pp. 734–739.
[27] Kwon Y.S., Kim J., and Lee I.M., Clogging Theory - Based Real Time Grouting Management System for Underwater Tunnel, Geomech. Eng., Vol. 16, Issue 2, 2018, pp. 159–168.